I&EC research
Industrial & Engineering Chemistry Research

pubs.acs.org/IECR

Article

Fine-Tuning of Particle Size and Morphology of Silica Coated Iron Oxide Nanoparticles

Zeeshan Ali, Jens-Petter Andreassen, and Sulalit Bandyopadhyay*

Cite This: *Ind. Eng. Chem. Res.* 2023, 62, 4831−4839

Read Online

ACCESS | Metrics & More | Article Recommendations | Supporting Information

ABSTRACT: Due to their unique properties such as superparamagnetism, easy surface functionalization, and colloidal stability among others, silica coated iron oxide nanoparticles (SIONPs) have received remarkable attention for biomedical applications such as in diagnostics or therapeutics. Tuning the particle size and size distribution of SIONPs as a function of solvent, catalyst, silica precursor, etc., in a modified Stöber's method has been extensively studied. However, there has been no concerted effort to study the effect of the above parameters along with the surface chemistry of the iron oxide nanoparticles (IONPs) on the morphologies obtained and hence the resultant magnetic properties. Here, we report an in-depth investigation of the nature of solvent, concentration of catalyst, mass ratio of IONPs to silica precursor and surface groups of IONPs on the size and resultant morphology of SIONPs. We report here for the first time the evolution of different morphologies, namely, fused, irregular, aggregate, and spherical morphologies, by careful control of the reaction conditions. Controlling the sizes and morphologies exerts an influential effect on the resultant magnetic properties and, thus, their applications downstream.

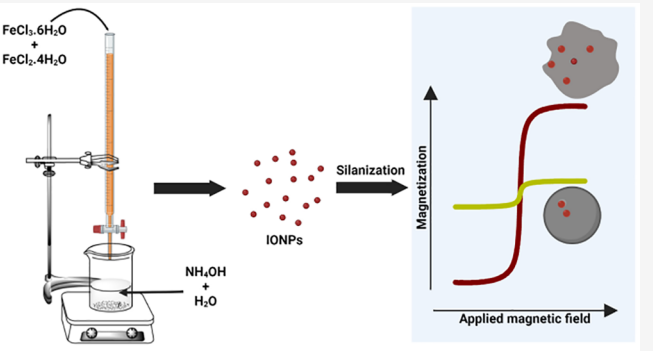

INTRODUCTION

Recent years have seen an exponential growth in research on nanomaterials in biomedicine with applications ranging from contrast agents in medical imaging to carriers for gene delivery.[1] Among these, iron oxide nanoparticles (IONPs) find extensive applications in novel diagnostics, drug delivery, magnetic resonance imaging (MRI), protein purification, and so on because of their unique properties such as superparamagnetism, tunable surface chemistry, and low cytotoxicity among others.[2] To warrant their use in these aforementioned applications, they should possess high magnetic saturations, overall narrow particle size distributions (PSDs), and high colloidal stability, all of which may be controlled by tuning their synthesis methods.[3] Among various strategies, the coating of IONPs with inorganic material, in particular silica, is an effective method for fine-tuning their magnetic saturation by controlling interparticle interactions. In addition, a silica coating offers possibilities to further functionalize their surfaces with various biomarkers by exploiting the silanol groups on the surface.

Different methods such as sol−gel, aerosol pyrolysis, ion exchange, ion implantation, and melt quenching, are well reported for the synthesis of silica nanoparticles (SNPs) among which the Stöber's method (sol−gel based) is very popular due to its low processing temperature. The Stöber's method may be further modified to synthesize silica coated iron oxide nanoparticles (SIONPs). Successful application of SIONPs for magnetic sample preparation in biodiagnostics, such as in nucleic acid extraction or protein extraction or the likes thereof, depends on further understanding the correlation between size, morphology and magnetic saturation of SIONPs as a function of various reaction conditions. Stöber's method involves the hydrolysis and condensation of silica precursor producing SNPs for which the particle size and morphology are dependent on the nature of the solvent, concentration of the catalyst, and silica precursor among other reaction conditions, but for SIONPs, an additional factor also comes into play, primarily, concentration of the IONPs and functional groups on their surface.

Although one is able to find several reports that discuss the roles of the above-mentioned reaction parameters in controlling the sizes of SNPs, not many works discuss their role in the synthesis of SIONPs. Interestingly, even these reports have investigated the effects within a narrow range of the parameters, and no concerted efforts have been made to elucidate how and why these parameters affect the resulting morphologies.[4−15] These reports also point to two main morphologies—spherical

Received: September 19, 2022
Revised: February 23, 2023
Accepted: March 1, 2023
Published: March 14, 2023

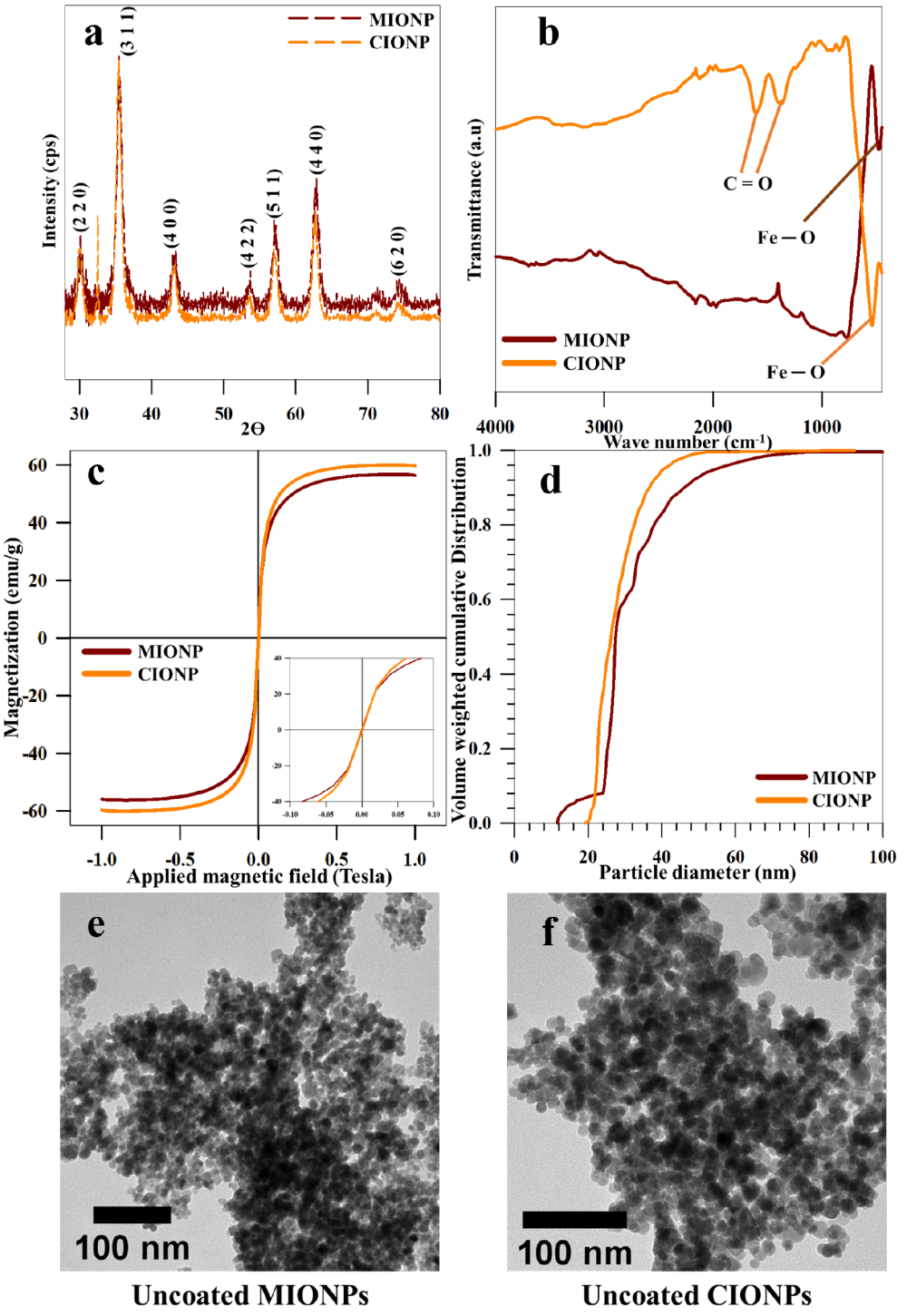

Figure 1. Characterization of IONPs. (a) XRD pattern of IONPs: the Miller indices and *d* spacings of the corresponding reflections are shown; (b) FT-IR spectra of IONPs; (C) hysteresis loops of IONPs measured through VSM; (d) PSDs of IONPs measured using the LUMiSizer; (e) representative TEM image of uncoated MIONPs; (f) representative TEM image of uncoated CIONPs.

and aggregated particles for both SNPs and SIONPs, with limited understanding of their impacts on resulting magnetic properties. Therefore, an in-detail scanning of the variable space to correlate their impacts on sizes, size distributions, morphologies, and resulting magnetic properties of SIONPs was chosen to be the focus of this work. Here, we have systematically investigated the effect of nature of solvent, mass ratio of IONPs to silica precursor, concentration of ammonium hydroxide, and surface chemistry of IONPs on the sizes, morphologies, and subsequently the magnetic properties of SIONPs. Our understanding will guide a better design of particles resulting in tailored physicochemical properties.

RESULTS AND DISCUSSION

IONPs were synthesized using the coprecipitation method and thereafter coated with a silica shell by varying reaction

https://doi.org/10.1021/acs.iecr.2c03338
Ind. Eng. Chem. Res. 2023, 62, 4831−4839

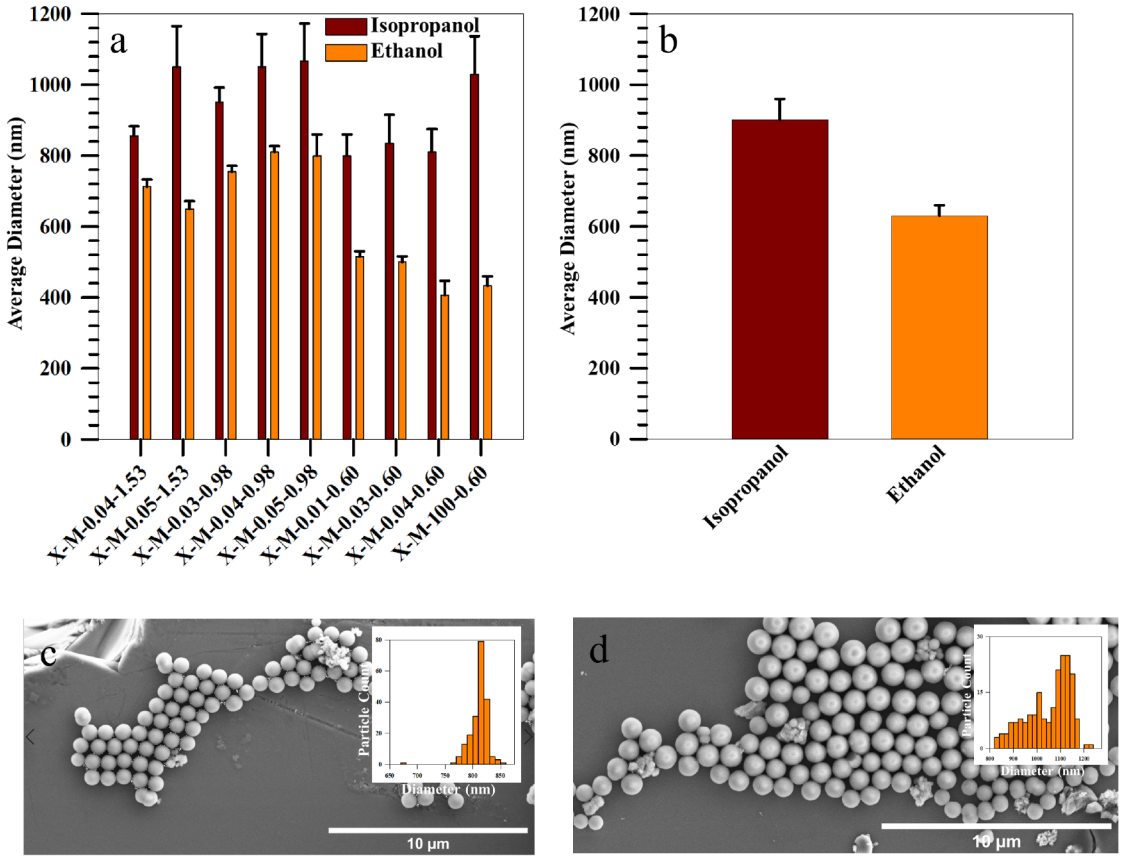

Figure 2. Effect of solvent. (a) Average diameter of SIONPs in ethanol and isopropanol; (b) overall average diameter of SIONPs in both solvents; (c) representative SEM image of E-M-0.04-0.98 and its PSD inset; and (d) representative SEM image of I-M-0.04-0.98 and its PSD inset.

parameters such as nature of solvent, concentration of ammonium hydroxide, and mass of IONPs. Herein, we present the characterization data for IONPs, followed by the effect of reaction parameters on size and morphology of SIONPs followed by a discussion on the resultant magnetic properties.

Characterization of IONPs. Two different types of IONPs, namely MIONPs and CIONPs, were used in this study, both being synthesized using coprecipitation and the latter being synthesized in the presence of citric acid. The crystallinity, surface functional groups, magnetic properties, and PSDs of these IONPs were characterized using XRD, FTIR, VSM, and Lumisizer, respectively. Figure 1a shows diffraction patterns of MIONPs and CIONPs for which major diffraction peaks for both XRD patterns are attributed to (2 2 0), (3 1 1), (4 0 0), (4 2 2), (5 1 1), (4 4 0), and (6 2 0) reflections of inverse cubic spinel structure of Fe_3O_4 as also reported in the literature.[16,17] These findings show that the coating of the IONPs surface with the citrate ligand did not change the crystalline nature of the magnetite nanoparticles.

To study the functional groups on the surfaces of MIONPs and CIONPs, the particles were characterized using FT-IR spectroscopy over a range of 4000−500 cm^{-1} as shown in Figure 1b. It can be seen that the peak at 3368 cm^{-1} shows the stretching vibrations of −OH groups, and the peak around 600 cm^{-1} represents the Fe−O stretching. The peaks at 1587 and 1408 cm^{-1} in the FT-IR spectrum of CIONPs represent the asymmetric and symmetric C═O bonds, respectively, that confirms the citrate coating of CIONPs. These IR spectra also match the findings for these particles that have been reported in the literature.[16,18]

The magnetic hysteresis loops of MIONPs and CIONPs were measured using VSM, and Figure 1(c) shows the magnetization versus magnetic field at 300 K obtained by cycling the field between −1 and 1 T for both MIONPs and CIONPs. A negligible coercivity and remanence in the hysteresis loops indicate the superparamagnetic nature of both the nanoparticles (NPs). The saturation magnetization (M_s) of MIONPs and CIONPs was measured to be 56 emu g^{-1} and 59 emu g^{-1}, respectively, which are representative of similar IONPs previously reported in the literature.[19]

Volume weighted median diameters of MIONPs and CIONPs were measured using an analytical centrifuge—LUMiSizer. Both IONPs showed median diameters of ≈27 nm, while the PSD for CIONPs was observed to be narrower than that of MIONPs as can be seen in Figure 1d. The difference in PSDs may be attributed to the fact that the presence of citrate groups on the surface of CIONPs, as also confirmed from FTIR spectra, helps reduce aggregation in dispersion and provides higher colloidal stability. Higher colloidal stability of CIONPs is further confirmed by higher zeta potential values of −47 mV compared to −34 mV in the case of MIONPs. Figure 1e and Figure 1f show the representative TEM images for the morphologies of uncoated MIONPs and CIONPs, respectively. MIONPs and CIONPs, possessing similar crystal structure, magnetic properties, and sizes while differing in size distributions, have been used as cores for growing silica shells

https://doi.org/10.1021/acs.iecr.2c03338
Ind. Eng. Chem. Res. 2023, 62, 4831−4839

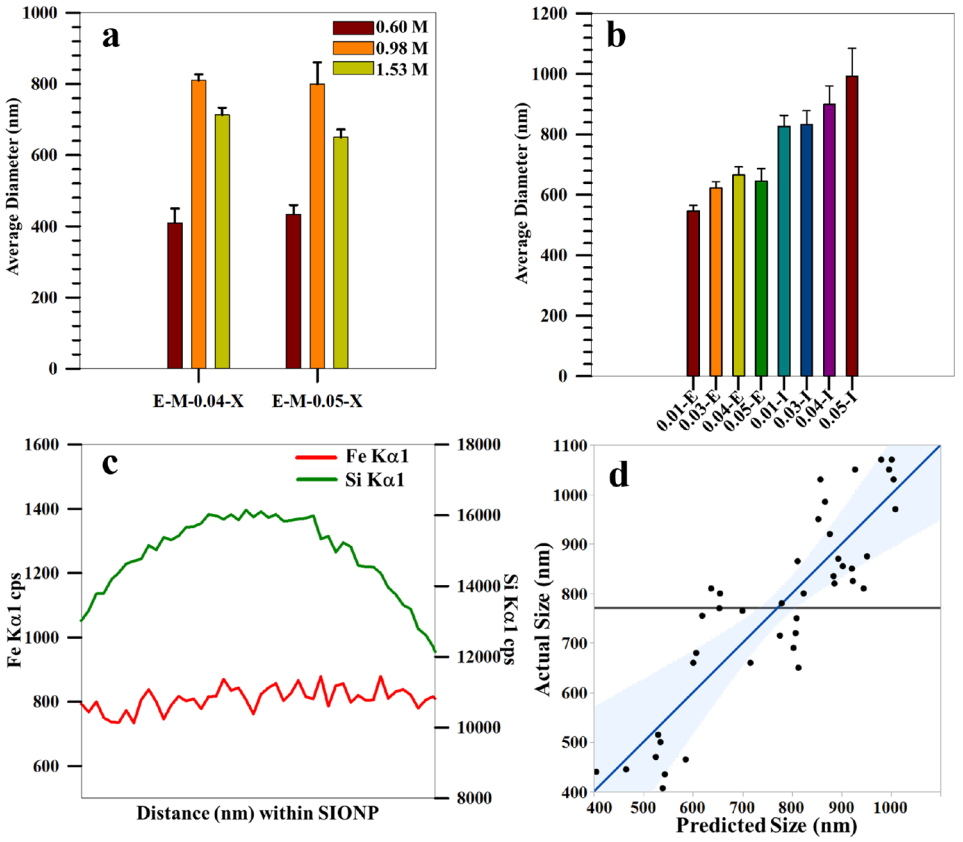

Figure 3. Characterization of SIONPs. (a) Effect of ammonium hydroxide concentration represented by change in average SEM diameter of SIONPs; (b) effect of mass ratio of IONPs and TEOS on particle diameter of SIONPs; (c) EDX line spectrum of sample S55; and (d) statistical model fitting using JMP software.

in order to understand the effects of this and other reaction parameters on the resultant NPs.

Effect of Reaction Parameters. This section discusses the effect and significance of important reaction parameters on the particle size, morphology, and magnetic properties of SIONPs during silica coating of IONPs through the modified Stöber's method.

Effect of Solvent. Figure 2a shows the average SEM sizes of the SIONPs synthesized in ethanol and isopropanol solvents for different synthesis conditions. The darker bar represents the average size in isopropanol, while the lighter bar represents the average size in ethanol for otherwise identical reaction conditions. The error bars represent the standard deviations of the size distributions. An overview observation shows that SIONPs obtained using isopropanol as the solvent have a higher SEM size compared to their homologue sample in ethanol. Here, it must be noted that all samples studied show individual spherical particles and also aggregate morphologies (Supporting Information: section 6), which has been overlooked in the literature. However, in our samples, these aggregate structures are the minority population (except when mentioned specifically), and hence, all our size analysis has been based on measuring spherical particles from representative SEM images. The solvent effect is further exemplified by Figure 2b which represents average SEM diameters of all the different SIONPs synthesized in ethanol and isopropanol solvents, respectively. Figure 2 panels c and d show the representative SEM images with their PSD inset for two similar synthesis conditions only differing in solvent used, ethanol, and isopropanol, respectively. SEM images reflect the spherical nature of the SIONPs in both cases with a distinctively broader size distribution in the case of isopropanol, for this particular reaction condition. The difference in sizes of SIONPs in the two solvents may be explained by looking in detail into the reaction mechanism. The synthesis of SIONPs is assumed to take place as a two-step process. In the first step, silica precursor (TEOS) is hydrolyzed through a nucleophilic substitution reaction caused by the hydroxy groups (from the solvent or the surface of IONPs) to form a transition state complex, i.e., silanol monomers in which ethoxy groups are replaced with the hydroxy groups as shown in eq 1. In the second step, these monomers condense to form a network of silica shown by eq 2 and then make a film of silica over the IONPs surface. Since, synthesis of silanol monomers is a nucelophilic substitution reaction as shown in eq 1, the nature of the solvent is an important parameter primarily because alcoholic solvents affect the nucleophilicity of the hydroxyl group through hydrogen bonding and increase its stability that subsequently lowers the rate of the hydrolysis step. A high polar solvent will form stronger hydrogen bonding with the hydroxy groups and slow down the hydrolysis of TEOS. Since isopropanol is less polar than ethanol, it translates to a higher hydrolysis rate and higher particle size of SIONPs. Molecular weight of the alcohols is also a significant parameter for this reaction, since it may be easily related to the polarity and dielectric constant: a higher molecular weight alcohol has lower polarity and dielectric constant. As the polarity increases, the particle size of SIONPs decreases, since the particles tend to aggregate easily in less polar solvents resulting in increased particle size. The dielectric

https://doi.org/10.1021/acs.iecr.2c03338
Ind. Eng. Chem. Res. 2023, 62, 4831−4839

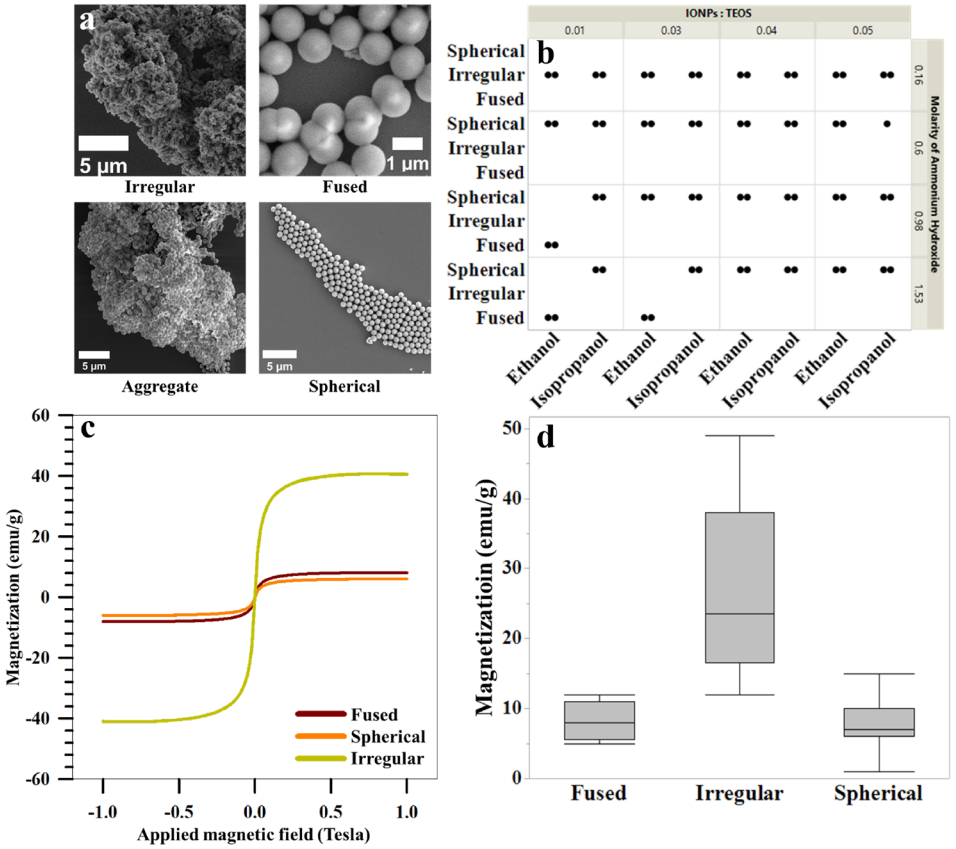

Figure 4. Effect of reaction parameters on morphology of SIONPs. (a) Four different morphologies of SIONPs observed in this study; (b) morphologies associated with various reaction parameters during silanization; (c) hysteresis loops of different morphologies of SIONPs measured using VSM; (d) average magnetization of various morphologies of SIONPs in the whole data set.

constant and Debye length κ are inversely related to each other in a colloidal suspension, hence according to DLVO theory, larger particles should result due to aggregation in a solvent medium having lower dielectric constant. At higher dielectric constant, the static repulsive forces between the particles are higher than the attractive van der Waals forces which prevent their aggregation to form larger particles, which results in a lower final particle size of SIONPs.

$$\mathrm{Si(OEt)_4} + x\mathrm{H_2O} \rightleftharpoons \mathrm{Si(OEt)_{4-x}(OH)_x} + x\mathrm{EtOH} \quad (1)$$

$$2\mathrm{Si(OEt)_{4-x}(OH)}x \rightleftharpoons (\mathrm{EtO})_{8-2x}(\mathrm{Si-O-Si})(\mathrm{OH})_{2x-2} + \mathrm{H_2O} \quad (2)$$

Effect of Ammonium Hydroxide. In this study, four concentrations of ammonium hydroxide, i.e., 0.16 M, 0.60 M, 0.98 M, and 1.53 M were used during the experiments. Figure 3a shows the changes in the average SEM sizes of SIONPs as a function of the last three concentrations of the catalyst since at 0.16 M concentration, big irregular shaped particles of SIONPs were formed for which it was impossible to measure the diameter. As can be seen, the average diameter of SIONPs increases with an increase in the concentration of ammonium hydroxide from 0.60 to 0.98 M and then decreases with a further increase in the concentration to 1.53 M. Although the data shown here is compiled for those SIONPs that are synthesized using MIONPs, a similar trend is observed in the case of SIONPs synthesized using CIONPs, but it does not reduce significantly. The hydrolysis of TEOS involves substitution of ethoxyl groups (-Si-OEt) with the OH^- ions; therefore, an increase in the ammonium hydroxide concentration increases the rate of hydrolysis of TEOS owing to an increase of OH^- ions concentration which contributes to a higher number of silanol monomers in the system. Similar to hydrolysis, the condensation of silanol monomers to form silica networks is also accelerated, since the silica monomers become more positively charged due to deprotonation. Then, these silica networks make a silica film on the IONPs' surface resulting in higher particle sizes of SIONPs. At an ammonium concentration > 0.98 M at high pH, nucleation is believed to take place in the initial stages of the reaction, and after that the monomers become highly negatively charged and become stable. They prefer to condense to form silica networks instead of nucleating to form new monomers, which results in shorter silica networks and hence smaller sizes of SIONPs. Hence, it is hypothesized that increasing the concentration from 0.98 to 1.53 M increases the hydrolysis rate of TEOS, and subsequently, the rate of condensation of silanol monomers becomes the rate limiting step. Hence, it results in the synthesis of less silanol monomers, which decreases the number of particles produced by condensation of silanol monomers, since the presence of less number of particles to deposit on each other reduces the particle size of the SIONPs.

Effect of IONPs: TEOS Mass. The final parameter that has been varied in our study is the mass ratio of IONPs to TEOS. The different ratios studied herein are 0.01, 0.03, 0.04, and 0.05. Figure 3b shows the effect of increase in ratios on average SEM sizes of SIONPs in both solvents. As can be observed, increase in the ratio of IONPs/TEOS usually does not affect significantly

https://doi.org/10.1021/acs.iecr.2c03338
Ind. Eng. Chem. Res. 2023, 62, 4831−4839

the average sizes of SIONPs when ethanol is used as the solvent, while the average diameters of SIONPs increase with the increase in the ratio of IONPs/TEOS when isopropanol is used as the solvent. It is hypothesized that aggregation of IONPs causes an increase in the size of SIONPs during silanization in isopropanol as has been highlighted in analyzing the effect of solvents. Since isopropanol has lower molecular weight and polarity than ethanol, IONPs tend to aggregate in isopropanol which is believed to increase the sizes of SIONPs. Figure 3c shows the EDX line spectrum of the sample S55 (Table S1: Supporting Information) and confirms the presence of Fe and Si (SEM image is represented in the Supporting Information: Figure S1. The presented EDX line spectrum refers to line 29 in the SEM image). The exact distribution of the IONPs within the silica matrix has not been the focus here. Our results combined show that the sizes of the SIONPs can be effectively controlled by tuning the studied reaction parameters.

Statistical Analysis. To determine the significance and interplay of these above-discussed reaction parameters, the average SEM diameters of SIONPs were fitted into an effective screening model using JMP software that is represented in Figure 3d. The software performs root mean square error (RMSE) analysis in order to find the correlation between the predicted size and actual size of SIONPs. During this analysis, the nature of solvent, ratio of IONPs mass and TEOS, surface coating of IONPs, and concentration of ammonium hydroxide (M) were used as input variables, while the average SEM size of the SIONPS was treated as output variable. The RMSE analysis reflects the significance of these parameters by calculating the *p*-value for each input parameter. According to the model, the nature of the solvent is found to be the most statistically significant factor which affects the size of SIONPs while a change of the IONPs surface (MIONPs and CIONPs) is statistically the least significant factor with a *p*-value of 0.6. The concentration of ammonium hydroxide (M) proves to be the second most statistically significant factor which affects the size of SIONPs, with the *p*-value of 0.00023. According to the model fitting, R^2 was calculated to be 77% for this data, and the residual plot for this study (Supporting Information, Figure S2) is randomly distributed further confirming a good fit for this model. It should be mentioned that lower values for RMSE and R^2 could be because this model analyzed the data for only 0.6 M, 0.98 M, and 1.53 M concentration of ammonium hydroxide since it was not possible to measure the diameter of SIONPs at 0.16 M ammonium hydroxide concentration because of the irregular morphology of the SIONPs. In addition, the diameter of fused particles was not included in this statistical analysis. Although the statistical model helps us analyze the most significant reaction parameters, the significance should be interpreted as directly correlating to the largest deviations observed in the data sets, and this interpretation may differ from the actual mechanistic understanding of the formation of SIONPs.

Morphologies. Apart from particle size, the modified Stöber's method can also help to control the morphologies of SIONPs by controlling the above-discussed reaction parameters that can eventually give rise to different magnetic properties. Researchers have reported morphologies of SIONPs that look like aggregates of SIONPs or distinct spherical SIONPs.[5,20] The same is the case for SNPs for which researchers have reported either aggregated morphologies or spherical morphologies,[6,14] but SNPs and SIONPs can have other morphologies with specific size and magnetic properties that are being reported here and have not been of primary focus in the literature. Four distinct morphologies of SIONPs were observed in this experimental study as represented in Figure 4a, i.e., irregular, fused, aggregate, and spherical shaped SIONPs. Figure 4b maps the different obtained morphologies in relation to the reaction conditions to visualize the parameter space. Irregular SIONPs were formed when 0.16 M ammonium hydroxide was used during silanization in both solvents. Aggregates were observed in all the reactions when the concentration of ammonium hydroxide was higher than 0.16 M. Fused morphologies were observed when ethanol was used as solvent, and the concentration of ammonium hydroxide was 1.53 or 0.98 M ammonium hydroxide and the IONPs/TEOS mass ratio was lower. Spherical SIONPs were observed when the concentration of ammonium hydroxide was 0.62 M or higher in ethanol as well as in isopropanol. It is proposed that less hydrolyzed silanol monomers are synthesized at lower ammonium hydroxide concentration (0.16 M) which leads to formation of irregular shaped particles, while silanol monomers formed at high concentration of ammonium hydroxide are more hydrolyzed, growing in three-dimensional pattern that results in spherical shaped SIONPs. Ethanol has a lower molecular weight than isopropanol and offers lower steric hindrance during silanization, due to which they have high interparticle collisions that leads to synthesis of fused structures. Figure 4b further shows that nature of solvent and concentration of ammonium hydroxide are the significant factors for the synthesis of fused SIONPs. Control experiments were performed for both solvents and different concentrations of ammonium hydroxide without IONPs mass (Supporting Information: Figure S3). It was observed that mass ratio of IONPs/TEOS is the critical factor for fused SIONPs. The addition of IONPs in the reaction medium changes the morphology of bare silica particles to spherical particles in isopropanol, but in ethanol, it still gives fused particles when the ratio of IONPs and TEOS is less than 0.04 and the concentration of ammonium hydroxide is higher than 0.6 M. It is proposed that silica particles do not have enough IONPs surface available to grow on, so fused SIONPs are formed, but when the mass of IONPs is increased, then spherical SIONPs are formed. Thus, the studied reaction parameters not only influence the sizes and size distributions of SIONPs, but also help in crafting out specific parameter spaces, where one type of morphology dominates over the others.

Saturation Magnetization of SIONPs. Figure 4 panels c and d represent the hysteresis loop and average magnetization of various morphologies of SIONPs observed in this study, respectively. It should be mentioned that the saturation magnetization in Figure 4c and 4d is expressed in emu g^{-1} of SIONPs. As observed for IONPs, the magnetization curves for SIONPs show negligible coercivity and remanence in the hysteresis loops indicating the superparamagnetic nature of SIONPs. The coating of MIONPs and CIONPs reduced their magnetic saturations because of the presence of a nonmagnetic silica shell since all the samples showed their saturation magnetization less than the bare IONPs presented in Figure 1c. Figure 4c shows that spherical and fused SIONPs have similar magnetic saturations but irregular shaped particles have higher magnetic saturations. It is proposed that irregular shaped particles may have not been successfully coated with silica shell and might have bare IONPs which gives them higher magnetic saturation values. For their applications in diagnostics, although higher magnetic saturation is desirable particle size and morphology also play an important role. Our study therefore shows that by fine-tuning the reaction parameters, it is not only

https://doi.org/10.1021/acs.iecr.2c03338
Ind. Eng. Chem. Res. 2023, 62, 4831−4839

possible to fine-tune the sizes and size distributions of the SIONPs, but also obtain insights into how these reaction parameters can influence the morphology of SIONPs, further controlling their resultant magnetic properties.

CONCLUSION

Herein, we have reported the effects of reaction parameters such as nature of solvent, catalyst, surface coating of IONPs, mass ratio of IONPs to silica precursor on the formation of SIONPs using a modified Stöber's method. Two different IONPs of similar sizes, crystalline structure, and magnetic properties, varying only in surface functional groups, hydroxyl (MIONPs) and citrate (CIONPs), were synthesized using coprecipitation. During the silica coating of the IONPs, sizes of the resultant SIONPs are observed to be significantly affected by the solvent, isopropanol giving larger sizes compared to ethanol. The concentration of the catalyst, ammonium hydroxide, is observed to play a pivotal role in controlling the shape evolution of the SIONPs. Concentrations above 0.16 M are required for avoiding irregular structure formation. Subsequently, our approach has culminated in mapping the parameter space, whereby with a careful tuning of the reaction parameters, four different morphologies, namely, spherical, fused, irregular, and aggregate, are being reported for the first time. It is worthy of mention that these morphologies possess different magnetic saturations while still retaining their superparamagnetic behaviors. Therefore, our results form the basis of a systematic parameter−property mapping for control of particle size, morphology, and resultant magnetic properties, thereby allowing the fine-tuning of SIONPs for a wide array of biomedical applications.

EXPERIMENTAL SECTION

Materials. Iron(II) chloride tetrahydrate ($FeCl_2.4H_2O$, ≥99%), Iron(III) chloride hexahydrate ($FeCl_3.6H_2O$, ≥99%), tetraethyl orthosilicate (TEOS, reagent grade 98%), ammonium hydroxide solution (NH_4OH, 25 wt %), and citric acid (reagent grade, ≥99.5%) were purchased from Sigma-Aldrich (Schnelldorf, Germany) for this study. 2-Propanol (technical grade ≥98%), and ethanol (96 vol %) were bought from VWR chemicals (France). All these chemicals were used as received from the suppliers without any purification or modification. All solutions were prepared using Milli-Q water, having a resistivity ∼18.2 MΩ/cm at 25 °C, taken from an Arium (Göttingen, Germany) water purification system.

Synthesis of IONPs. The synthesis process has been adapted from our previously reported study.[21] IONPs were synthesized via chemical coprecipitation. Briefly, 84.6 mg of MQ water was weighed in a beaker, and 15.4 mL of 25% (wt) NH_4OH solution was added to it to prepare a 1 M solution. 8.0 g of $FeCl_2{\cdot}4H_2O$ and 21.6 g of $FeCl_3{\cdot}6H_2O$ were weighed and dissolved in 100 mL of MQ water in a volumetric flask. 10 mL of this solution was added to 100 mL of 1 M ammonia solution dropwise (using a buret), with the reaction being kept under vigorous magnetic stirring. The final NPs were obtained using magnetic separation by three washing cycles with MQ water. The reaction was repeated four times, and the NPs obtained were mixed together to prepare a stock solution. These IONPs are represented as MIONPs in this study.

Citrate Coated IONPs. This method has been adapted and modified from the study by Nigam et al.[22] Briefly, 4.4 g of $FeCl_3{\cdot}6H_2O$ and 1.7 g of $FeCl_2{\cdot}4H_2O$ were dissolved in 80 mL of MQ water and transferred to a three-necked jacketed reactor, kept under inert atmosphere on a hot stirrer plate. The reaction mixture was kept under magnetic stirring at 1000 rpm for the entire duration. The temperature was slowly raised to 70 °C using water circulated from a Julabo water bath. After the temperature reached the set point, the reaction mixture was kept at the same temperature for 30 min before the instantaneous addition of 20 mL of 25% (wt) ammonium hydroxide solution. The temperature was maintained at 70 °C for another 30 min. Then, 4 mL of citric acid solution (0.5 g/mL) was added instantaneously. and the temperature was slowly raised to 90 °C and maintained for 60 min. The NPs were obtained using magnetic separation by three washing cycles with MQ water. These citrate coated IONPs are represented as CIONPs in this study.

Silica Coating of IONPs. Silica coating of IONPs was carried out by a modified Stöber's method. Briefly, IONPs were washed three times with the alcohol solvent (ethanol/isopropanol) using a permanent magnet and redispersed in 1 mL of alcohol solvent. Afterward, 19 mL of alcohol solvent was stirred at 600 rpm using a magnetic stirrer at room temperature, and TEOS was added. After 15 min, IONPs stock solution of 53 mg/mL was sonicated, and a calculated volume was added to the reaction medium followed by NH_4OH addition after another 15 min as per the specific reaction conditions (Supporting Information: Table S1). At the end of the reaction, SIONPs were washed with water and alcohol solvent several times through magnetic separation, and the final particles were redispersed in MQ water. These particles are further labeled as SIONPs. In the results section, the sample name has been chosen to denote the experimental conditions for easy discussion of the results. The sample name is composed of two alphabets followed by two digits. The first alphabet indicates the type of solvent used in the experiment ('E' ethanol and 'I' isopropanol). The second alphabet tells about the surface of IONPs ('M' IONPs without citrate coating and 'C' IONPs with citrate ligand coated on their surface). Next part of the sample name is the number which shows the mass ratio of IONPs and TEOS, and last number shows the molarity (M) of ammonium hydroxide in the reaction volume. For example; I-M-0.01-0.98 would show that isopropanol, IONPs without citrate ligand, 0.01 mass ratio of IONPs to TEOS, and 0.98 M ammonium hydroxide solution are the reaction conditions in this specific experiment. 'X' indicates the parameter which is being discussed in a specific section.

Characterization Techniques. *Scanning Electron Microscopy.* SIONPs were imaged using FEI Apreo scanning electron microscope (SEM) at NTNU Nanolab cleanroom facilities, and these SEM images were used further to measure the size and particle size distribution (PSD) of the SIONPs using ImageJ. Samples for SEM analysis were prepared by cleaning a silicon wafer using plasma cleaner and dropping 10−15 μL of sample onto this wafer that was dried using a heating plate at 50 °C.

Transmission Electron Microscopy. Uncoated MIONPs and CIONPs were imaged using Thermo Fisher Tecnai 12 transmission electron microscope (TEM) with an accelerating voltage of 100 kV at the department of Clinical and Molecular Medicine NTNU. Samples for TEM imaging were prepared by dropping 40−50 μL of dilute suspensions of MIONPs and CIONPs onto carbon-coated copper grids.

Lumisizer. The multisample analytical centrifuge, LUMiSizer (L.U.M.GmbH, Berlin Germany), was used to characterize the particle size and PSD of two types of IONPs used in this study

https://doi.org/10.1021/acs.iecr.2c03338
Ind. Eng. Chem. Res. 2023, 62, 4831−4839

i.e., MIONPs and CIONPs. The measurement principle is based on Stokes' law and employs the STEP-technology (space- and time-resolved extinction profiles) to measure the intensity of the light as a function of time and position over the entire sample length during their sedimentation. The progression of the transmission profiles contains the information on the kinetics of separation of particles and allows particle size and PSD characterization.

Litesizer 500. The zeta potential of both MIONPs and CIONPs were measured using an Omega cuvette through Anton Paar Litesizer 500 instrument that determines the speed of particles in the presence of an electric field. The speed of the movement of the particles depends on their surface charge: the higher is the magnitude of zeta potential, the higher is the stability of the particles.

X-ray Diffraction (XRD). Crystallographic structures of both types of IONPs used in this study were investigated by X-ray powder diffraction (XRD) using a Bruker D8 Advance Da-Vinci equipped with a LynxEye detector working in Bragg−Brentano geometry. Diffraction patterns were recorded with Cu K radiation (Λ = 1.5406 Å), a step size of 2Θ = 0.045°, and an integration time of 1.28 s using a variable divergent slit. The samples were prepared by dropping SIONPs onto silicon wafers and dried using heating plate.

Attenuated Total Reflection-Fourier Transform Infrared (ATR-FTIR). The attenuated total reflection-Fourier transform infrared (ATR-FTIR) spectra were obtained using a Vertex 80v vacuum FTIR spectrometer. OPUS software was used to record spectra between 600 and 4000 cm^{-1} using 50 scans at a resolution of 4 cm^{-1}.

Vibrating-Sample Magnetometer (VSM). The magnetic properties of MIONPs, CIONPs, and SIONPs were determined using a VSM instrument named MicroMag 3900 at room temperature with maximum applied magnetic fields of ±1 T. The sample was dried overnight and put in a capsule and fixed using tape to avoid the movement of the NPs during the measurement.

■ ASSOCIATED CONTENT

Supporting Information

The Supporting Information is available free of charge at https://pubs.acs.org/doi/10.1021/acs.iecr.2c03338.

Experimental conditions for reactions conducted in this study; average SEM diameter, maximum magnetization and standard deviation of SIONPs; experimental design; residual plot; control experiments; representative SEM images (PDF)

Representative SEM images for all the reactions performed in the study (ZIP)

■ AUTHOR INFORMATION

Corresponding Author

Sulalit Bandyopadhyay − *Particle Engineering Centre, Department of Chemical Engineering, Norwegian University of Science and Technology, Trondheim 7491, Norway;* orcid.org/0000-0002-2918-286X; Email: sulalit.bandyopadhyay@ntnu.no

Authors

Zeeshan Ali − *Particle Engineering Centre, Department of Chemical Engineering, Norwegian University of Science and Technology, Trondheim 7491, Norway;* orcid.org/0000-0002-4170-670X

Jens-Petter Andreassen − *Department of Chemical Engineering, Norwegian University of Science and Technology, Trondheim 7491, Norway*

Complete contact information is available at: https://pubs.acs.org/10.1021/acs.iecr.2c03338

Notes

The authors declare no competing financial interest.

■ ACKNOWLEDGMENTS

The authors thank Regina Lopez Fyllingsnes for doing some initial measurements and Maximilian Clemens Winkler for some VSM measurements in this study. The authors also thank NorFab for the financial support in connection to the use of NTNU Nanolab and the Faculty of Natural Sciences and Technology, NTNU, for the financial support. We thank the Department of Chemical Engineering (NTNU) and Nanolab (NTNU), for all their financial, technical, and laboratory support.

■ REFERENCES

(1) Yen, S. K.; Padmanabhan, P.; Selvan, S. T. Multifunctional iron oxide nanoparticles for diagnostics, therapy and macromolecule delivery. *Theranostics* **2013**, *3*, 986.

(2) Ali, A.; Zafar, H.; Zia, M.; ul Haq, I.; Phull, A. R.; Ali, J. S.; Hussain, A. Synthesis, characterization, applications, and challenges of iron oxide nanoparticles. *Nanotechnology, science and applications* **2016**, *9*, 49.

(3) Gupta, A. K.; Gupta, M. Synthesis and surface engineering of iron oxide nanoparticles for biomedical applications. *biomaterials* **2005**, *26*, 3995−4021.

(4) Malay, O.; Yilgor, I.; Menceloglu, Y. Z. Effects of solvent on TEOS hydrolysis kinetics and silica particle size under basic conditions. *J. Sol-Gel Sci. Technol.* **2013**, *67*, 351−361.

(5) Pinho, S. L.; Pereira, G. A.; Voisin, P.; Kassem, J.; Bouchaud, V.; Etienne, L.; Peters, J. A.; Carlos, L.; Mornet, S.; Geraldes, C. F.; Rocha, J.; Delville, M.-H. Fine tuning of the relaxometry of γ-Fe2O3@ SiO2 nanoparticles by tweaking the silica coating thickness. *ACS Nano* **2010**, *4*, 5339−5349.

(6) Melnyk, I. Aminosilica nano-and submicrospheres: analysis of factors influencing morphology, structure and properties. *Chemistry Journal of Moldova* **2014**, *9*, 123−127.

(7) Dabbaghian, M.; Babalou, A.; Hadi, P.; Jannatdoust, E. A parametric study of the synthesis of silica nanoparticles via sol-gel precipitation method. *International Journal of Nanoscience and Nanotechnology* **2010**, *6*, 104−113.

(8) Wang, H.-C.; Wu, C.-Y.; Chung, C.-C.; Lai, M.-H.; Chung, T.-W. Analysis of parameters and interaction between parameters in preparation of uniform silicon dioxide nanoparticles using response surface methodology. *Industrial & engineering chemistry research* **2006**, *45*, 8043−8048.

(9) Matsoukas, T.; Gulari, E. Dynamics of growth of silica particles from ammonia-catalyzed hydrolysis of tetra-ethyl-orthosilicate. *J. Colloid Interface Sci.* **1988**, *124*, 252−261.

(10) Perchacz, M.; Beneš, H.; Kobera, L.; Walterová, Z. Influence of sol-gel conditions on the final structure of silica-based precursors. *J. Sol-Gel Sci. Technol.* **2015**, *75*, 649−663.

(11) Glaria, A.; Soule, S.; Hallali, N.; Ojo, W.-S.; Mirjolet, M.; Fuks, G.; Cornejo, A.; Allouche, J.; Dupin, J. C.; Martinez, H.; Carrey, J.; Chaudret, B.; Delpech, F.; Lachaize, S.; Nayral, C. Silica coated iron nanoparticles: synthesis, interface control, magnetic and hyperthermia properties. *RSC Adv.* **2018**, *8*, 32146−32156.

(12) Puscasu, E.; Sacarescu, L.; Lupu, N.; Grigoras, M.; Oanca, G.; Balasoiu, M.; Creanga, D. Iron oxide-silica nanocomposites yielded by

chemical route and sol-gel method. *J. Sol-Gel Sci. Technol.* **2016**, *79*, 457−465.
(13) Narayanan, T.; Reena Mary, A.; Anas Swalih, P.; Sakthi Kumar, D.; Makarov, D.; Albrecht, M.; Puthumana, J.; Anas, A.; Anantharaman, M. Enhanced bio-compatibility of ferrofluids of self-assembled superparamagnetic iron oxide-silica core-shell nanoparticles. *J. Nanosci. Nanotechnol.* **2011**, *11*, 1958−1967.
(14) Han, Y.; Lu, Z.; Teng, Z.; Liang, J.; Guo, Z.; Wang, D.; Han, M.-Y.; Yang, W. Unraveling the growth mechanism of silica particles in the stober method: in situ seeded growth model. *Langmuir* **2017**, *33*, 5879−5890.
(15) Luo, X.; Dong, J.; Zhang, L.; Du, J.; Wang, H.; Gao, W. Preparation of silica micro spheres via a semibatch sol-gel method. *J. Sol-Gel Sci. Technol.* **2017**, *81*, 669−677.
(16) Talone, A.; Ruggiero, L.; Slimani, S.; Imperatori, P.; Barucca, G.; Ricci, M.; Sodo, A.; Peddis, D. Magnetic mesoporous silica nanostructures: investigation of magnetic properties. *Nanotechnology* **2020**, *31*, 465707.
(17) Er, E. Ö.; Akkaya, E.; Özbek, B.; Bakırdere, S. Development of an analytical method based on citric acid coated magnetite nanoparticles assisted dispersive magnetic solid-phase extraction for the enrichment and extraction of sildenafil, tadalafil, vardenafil and avanafil in human plasma and urine prior to determination by LC-MS/MS. *Microchemical Journal* **2019**, *147*, 269−276.
(18) Qureashi, A.; Pandith, A. H.; Bashir, A.; Manzoor, T.; Malik, L. A.; Sheikh, F. A. Citrate coated magnetite: A complete magneto dielectric, electrochemical and DFT study for detection and removal of heavy metal ions. *Surfaces and Interfaces* **2021**, *23*, 101004.
(19) Cheraghipour, E.; Tamaddon, A.; Javadpour, S.; Bruce, I. J. PEG conjugated citrate-capped magnetite nanoparticles for biomedical applications. *J. Magn. Magn. Mater.* **2013**, *328*, 91−95.
(20) del Campo, A.; Sen, T.; Lellouche, J.-P.; Bruce, I. J. Multifunctional magnetite and silica-magnetite nanoparticles: Synthesis, surface activation and applications in life sciences. *J. Magn. Magn. Mater.* **2005**, *293*, 33−40.
(21) Sharma, A.; Foppen, J. W.; Banerjee, A.; Sawssen, S.; Bachhar, N.; Peddis, D.; Bandyopadhyay, S. Magnetic nanoparticles to unique DNA tracers: effect of functionalization on Physico-chemical properties. *Nanoscale Res. Lett.* **2021**, *16*, 1−16.
(22) Nigam, S.; Barick, K.; Bahadur, D. Development of citrate-stabilized Fe3O4 nanoparticles: conjugation and release of doxorubicin for therapeutic applications. *J. Magn. Magn. Mater.* **2011**, *323*, 237−243.

https://doi.org/10.1021/acs.iecr.2c03338
Ind. Eng. Chem. Res. 2023, 62, 4831−4839